ISSN 1063-7761, Journal of Experimental and Theoretical Physics, 2011, Vol. 112, No. 4, pp. 625–636. © Pleiades Publishing, Inc., 2011.
Original Russian Text © M.M. Otrokov, V.V. Tugushev, A. Ernst, S.A. Ostanin, V.M. Kuznetsov, E.V. Chulkov, 2011, published in Zhurnal Eksperimental'noi i Teoreticheskoi Fiziki, 2011, Vol. 139, No. 4, pp. 720–732.

ORDER, DISORDER, AND PHASE TRANSITION IN CONDENSED SYSTEM

Magnetic Ordering in Digital Alloys of Group-IV Semiconductors with 3*d*-Transition Metals

M. M. Otrokov[a], V. V. Tugushev[b,c], A. Ernst[d], S. A. Ostanin[d], V. M. Kuznetsov[a], and E. V. Chulkov[c,e]

[a] *Tomsk State University, Tomsk, 634050 Russia*
e-mail: otrokov@phys.tsu.ru
[b] *Russian Research Centre Kurchatov Institute, pl. Akademika Kurchatova 1, Moscow, 123182 Russia*
[c] *Departamento de Física de Materiales, Facultad de Ciencias Químicas, UPV/EHU and Centro de Física de Materiales (CFM) (CSIC- UPV/EHU), 20080 San Sebastián, Basque Country, Spain*
[d] *Max-Planck-Institut für Mikrostrukturphysik, D-06120 Halle, Germany*
[e] *Donostia International Physics Center (DIPC), 20018 San Sebastián, Basque Country, Spain*

Received August 10, 2010

Abstract—The ab initio investigation of the magnetic ordering in digital alloys consisting of monolayers of 3*d*-transition metals Ti, V, Cr, Mn, Fe, Co, and Ni introduced into the Si, Ge, and $Si_{0.5}Ge_{0.5}$ semiconductor hosts is reported. The calculations of the parameters of the exchange interactions and total-energy calculations indicate that the ferromagnetic order appears only in the manganese monolayers, whereas the antiferromagnetic order is more probable in V, Cr, and Fe monolayers, and Ti, Co, and Ni monolayers are nonmagnetic. The stability of the ferromagnetic phase in digital alloys containing manganese monolayers has been analyzed using the calculations of magnon spectra.

DOI: 10.1134/S1063776111030137

1. INTRODUCTION

Diluted magnetic semiconductors (DMSs) A^{IV}:M based on Group-IV elements (A^{IV} = Si, Ge) doped with magnetic 3*d*-transition metals (M = Cr, Mn, Fe, Co) have attracted large interest in recent years as new materials of magnetic electronics used, e.g., for spin injection [1]. On the one hand, such DMSs can be easily integrated in the standard technology of silicon-based nonmagnetic semiconductor structures. On the other hand, the efficient transport of spin-polarized charge carriers (as a rule, holes) can likely be successfully implemented in them. The most theoretical and experimental advance has been achieved in studying Ge/Mn and Si/Mn DMSs, although their magnetic and transport properties are still far from complete understanding.

According to the traditional terminology, Ge/Mn and Si/Mn DMSs are disordered alloys (solid solutions) $Ge_{1-x}Mn_x$ and $Si_{1-x}Mn_x$ with low or moderate ($x \approx 0.001$–0.1) concentrations of manganese. The ab initio calculations of the electronic structure reported in [2] indicate that the ferromagnetic ordering in such alloys occurs at sufficiently high Curie temperatures ($T_C \approx 300$–500 K). This ordering is caused by the indirect exchange of local moments on manganese ions through free carriers (holes) whose sources are manganese ions (carrier mediated ferromagnetism). The effective moment on a manganese ion should be $\mu \approx 3\mu_B$, slightly depending on the position occupied by this ion (we recall that the most energetically favorable position for an isolated manganese ion is a substitutional site in the germanium lattice or a tetrahedral interstitial site in the silicon lattice). The situation in real $Ge_{1-x}Mn_x$ and $Si_{1-x}Mn_x$ alloys appeared to be much more complex than that assumed in the model developed in [2] and the problem of high-temperature ferromagnetism in these alloys remains open. The reason is that any method of their growth is characterized by the strong phase segregation with the formation of various inclusions and clusters; this circumstance leads to contradiction between the experimental results and theoretical predictions for macroscopically homogeneous systems.

The nature of ferromagnetism in $Ge_{1-x}Mn_x$ alloys has not yet completely determined, although the existing experimental situation is clearly understood. In particular, epitaxial $Ge_{1-x}Mn_x$ ($x \approx 0.035$) films were studied in [3], where a ferromagnetic order was observed below $T = 116$ K; this order is likely due to the presence of magnetic inclusions (precipitates) with sizes from 2 to 6 nm where the concentration of manganese is higher than that in the main material. Investigations of alloys with the low or moderate concentrations of manganese ($x \approx 0.02$–0.1) [4–7] show that precipitates contain various manganese germanates such as Ge_3Mn_5 or Ge_8Mn_{11}, which have a short-range ferromagnetic order at temperatures near and above room temperature. This circumstance is responsible for the superparamagnetic behavior of precipitates, each having a giant magnetic moment (up to

TH-2011-15

$2000\mu_B$), observed in experiments above a certain characteristic blocking temperature. In order to consistently interpret the results of magnetic measurements in alloys with low and moderate concentrations of manganese ($x < 0.09$), the authors of [8] introduced two different ferromagnetic ordering temperatures, T_C^* and T_C, where the higher temperature $T_C^* \approx 300$ K corresponds to the appearance of the short-range ferromagnetic order inside a precipitate and the lower temperature $T_C \approx 10$ K is the point of the percolation transition to the ferromagnetic state throughout the sample. However, the ferromagnetic order at room temperature was observed in $Ge_{0.94}Mn_{0.06}$ [9] and $Ge_{0.981}Fe_{0.019}$ [10]. It was emphasized in [9, 10] that manganese and iron ions are incorporated into the germanium lattice, whereas no secondary phases and clusters were observed. The transport measurements reported in [11] revealed the semiconductor conductivity type in the $Ge_{0.81}Mn_{0.13}Fe_{0.06}$ alloy throughout the investigated temperature interval. According to the results of that work, the indirect ferromagnetic interaction is ensured by localized holes with a density of about 10^{20} cm^{-3} and a mobility of about 10 cm^2/(V s).

Thus, magnetic ordering in $Ge_{1-x}Mn_x$ alloys apparently occurs in several stages. At high temperatures (above or near room temperature), the short-range ferromagnetic order is formed inside individual nanoprecipitates, which appear as a result of large-scale fluctuations of the composition of an alloy and contain manganese germanates or solid solutions with an increased concentration of manganese. Then, at lower temperatures, blocking and possibly partial ordering of magnetic moments of these nanoprecipitates in the $Ge_{1-x}Mn_x$ matrix with a decreased concentration of manganese occur. Finally, at low temperatures, the process of the ferromagnetic ordering of the local moments of manganese ions dispersed in the $Ge_{1-x}Mn_x$ matrix begins, possibly through the percolation scenario (see, e.g., discussion in [5]).

The situation with understanding of the nature of ferromagnetism in $Si_{1-x}Mn_x$ alloys, for which the experimental results are very contradictory, is much more uncertain. There are data on the high-temperature ferromagnetic order ($T_C^* \approx 250$–400 K) in $Si_{1-x}Mn_x$ alloys with low or moderate concentrations of manganese ($x \approx 0.001$–0.1) obtained by the methods of vacuum deposition [12], ion implantation [13], and magnetron sputtering [14, 15] of manganese, but the mechanism of this ordering remains unclear. At the same time, the ferromagnetic order was not observed in α-$Si_{1-x}Mn_x$ alloys ($0.01 < x < 0.175$) obtained by manganese doping of amorphous silicon with the subsequent homogenization of an alloy [16], although the magnetic susceptibility of these alloys in a wide range of compositions satisfies the Curie–Weiss law with a very low effective moment (less than $0.1\mu_B$/Mn). The authors of [16] assumed that only a small part of the total number of manganese ions that are present in the silicon lattice in the form of isolated centers with local magnetic moments are involved in the formation of the ferromagnetic order in α-$Si_{1-x}Mn_x$ alloys, whereas the overwhelming majority of manganese ions are in nonmagnetic configurations. The results of X-ray [17, 18] and electron [19] microscopy indicate that most manganese ions do not occupy substitutional or interstitial sites in the silicon lattice, but enter in various silicides (such as Mn_4Si_7 or $Mn_{11}Si_{19}$), which form nanoclusters or nanoinclusions (nanoprecipitates) with a nominal composition of $MnSi_{1.7}$ [20]. In this case, the average magnetic moment per manganese ion calculated from the data on the saturation of the magnetization in a high magnetic field is very low (about $0.21\mu_B$) in complete contradiction with the theoretical predictions made in [2]. The anomalous Hall effect with the pronounced hysteresis behavior indicating the presence of the ferromagnetic order was observed in [21] in $Si_{1-x}Mn_x$ films with a high concentration of manganese ($x \approx 0.35$), which were obtained by the laser sputtering method. The Curie temperature $T_C \approx 250$ K and the effective moment per manganese ion $\mu \approx (0.1$–$0.2)\mu_B$ were determined. However, we emphasize that the system considered in [21] exhibits the metallic conductivity type and, thereby, is strongly different from the above-discussed systems with the semiconductor conductivity type [12–15]. In addition, the anomalous Hall effect was also observed in $Si_{1-x}Fe_x$ epitaxial films with $x \approx 0.07$ at temperatures below 26 K; this circumstance indicates the absence of high-temperature ferromagnetism in this material [22].

In view of the results reported above, serious problems concerning the nature of ferromagnetism in $Si_{1-x}Mn_x$ arise. On the one hand, the model of the indirect exchange between local moments on manganese ions by a carrier mediated ferromagnetism mechanism cannot evidently explain the appearance of the ferromagnetic order in these systems, because the number of such moments is very small. On the other hand, although the aforementioned manganese silicides are weak itinerant ferromagnets, it is very difficult to interpret the ferromagnetic order in $Si_{1-x}Mn_x$ alloys in the framework of the traditional mechanism of itinerant ferromagnetism. The reason is that the Curie temperature for most of known manganese silicides is $T_C \approx 50$ and the effective moment per manganese ion is $\mu \approx 0.01\mu_B$ [23, 24]; i.e., these values are an order of magnitude lower than the respective values in the systems under discussion. In recent work [25], it was assumed that ferromagnetism in $Si_{1-x}Mn_x$ alloys is not directly attributed to the presence of magnetic manganese ions in a certain form, but is caused by the appearance of magnetic defects (such as dangling bonds in the silicon lattice) in the process of the preparation of an alloy, e.g., by ion implantation or laser sputtering on a substrate. Thus, the problem of the nature and mecha-

nism of the ferromagnetic order in $Si_{1-x}Mn_x$ alloys remains unsolved.

Digital magnetic alloys (DMAs) A^{IV}/M considered in this work constitute a nontraditional type of DMSs based on Group-IV elements (hereinafter, marked as A^{IV}). In these materials, M ions (most often, manganese) with the nominal concentration corresponding to the mono- or submonolayer coverage are introduced to the Group-IV semiconductor (Si or Ge) by means of selective doping in the process of molecular beam epitaxy and form the so-called magnetic δ-layers [1]. These δ-layers form either individual magnetic elements of a hybrid semiconductor heterostructure or a periodic lattice of these elements (called the DMA). In this way, it is possible to reach a locally high concentration of ions of transition metals, which is much higher than their solubility limit in bulk semiconductors. The exchange interaction between the magnetic moments inside δ-layers is much stronger than that in bulk DMSs and the magnitude of the exchange interaction between δ-layers can be varied by choosing the composition and geometric parameters of DMAs. Therefore, the magnetic and transport properties of these materials can be varied in a wide range.

DMAs of the III–V/M type, where III–V = GaAs, GaSb, have been most actively investigated in recent years, primarily because reliable methods for obtaining relatively high-quality ferromagnetic δ-layers have been developed for these systems. In particular, a DMA in the form of a GaAs/MnAs heterostructure was grown by means of the alternating deposition of GaAs and MnAs nanolayers [26, 27]. In GaAs/Mn and GaSb/Mn DMAs, manganese ion submonolayers were periodically introduced into a GaAs or GaSb matrix [28, 29]. An original method for creating single ferromagnetic δ-layers of manganese ions in GaAs-based heterostructures, which was successfully implemented in [31, 32], is also worth noting. Despite very interesting prospects, A^{IV}/M DMAs remain almost unstudied experimentally. The problems of phase segregation (formation of silicides and germanates of transition metals in the process of the growth of DMAs) apparently prevent the growth of high-quality δ-layers in silicon and germanium matrices. The first success in this direction was achieved in [33] for $[Si(20\ Å)/Mn(x)]_{30}$ multilayer structures with the nominal δ-layer concentrations $x = 1$, 1.5, and 2.0 Å.

The main theoretical attention was focused on ab initio calculations of the band structure of A^{IV}/M DMAs considered in this work. The electronic spectrum of these DMAs contains both strongly correlated narrow bands and weakly correlated wide bands. The magnetic order inside each layer appears due to the strong correlation between electronic states in narrow bands and their hybridization with states in wide bands, i.e., occurs through the Anderson–Hubbard band mechanism [34]. At the same time, the exchange coupling between neighboring layers of transition metals has the pronounced character of superexchange and occurs by the tunneling of quasiparticles through quasi-two-dimensional spin-polarized states [35–38] formed by layers in the Group-IV element matrix.

2. FORMULATION OF THE PROBLEM

The ab initio investigations of the electronic structure and magnetic order of A^{IV}/M DMAs are usually devoted to the consideration of ideal substitutional monolayers, and manganese is most often chosen as a magnetic component. In particular, both the ferromagnetic ordering in the manganese layer and a nearly half-metallic electronic structure were predicted for a Ge/Mn DMA with a thickness of germanium spacers up to 31 atomic layers (below, we use the notation Ge_{31}/Mn) [39, 40]. Introducing the Hubbard parameter $U = 2$ eV for the p states of Ge,[1] the authors of [41] predicted the half-metallic electron spectrum for Ge_7/Mn and the enhancement of a tendency to the formation of the ferromagnetic order in a metallic layer. The magnetic order and electronic spectrum in Si/Mn DMAs are qualitatively the same as those in Ge/Mn [42]. It is additionally known that the half-metallic state in Si_{15}/Mn remains unchanged in the presence of 25% of vacancies or silicon atoms (located at the sites of the lattice) [43]. The Si_{23}/M (M = Cr, Mn, Fe, Co) DMAs were recently investigated in [44], where the ferromagnetic order in the chromium monolayer and the antiferromagnetic order in the Fe and Co layers were reported; the results obtained for DMAs with the manganese δ-layer were in agreement with the calculations reported in [42]. The authors of [44] assumed a small effect of structural relaxations on the magnetic order in the layers of transition metals and considered unrelaxed DMAs. However, the authors of [45] found that iron δ-layers in completely relaxed Si_N/Fe ($7 \le N \le 19$) DMAs are ferromagnetic. Furthermore, the calculations of total energies predicted the ferromagnetic ordering in the iron layer introduced into the silicon matrix. The ferromagnetic order in 0.25, 0.5, and full interstitial manganese monolayer in the silicon matrix was predicted in [46]. However, the full spin polarization at the Fermi level was detected only in a system with 0.25 monolayer of manganese. According to the performed calculations, the presence of interstitial silicon atoms in the substitutional δ-layer leads to the loss of the half-metallic properties in view of the energetically favorable exchange by positions, which leads to the occupation of a site by a silicon atom and of a tetrahedral void by a manganese atom.

It is worth noting that, in all aforementioned works except for [41], the type of the magnetic order was determined from the calculations of the total energies

[1] In the framework of the full-potential linearized augmented plane-wave method in the generalized gradient approximation to the exchange correlation functional, $U = 2$ eV ensures the experimental value of the fundamental gap in bulk germanium.

of the antiferromagnetic and ferromagnetic configurations of local moments in the δ-layer of a transition metal. The authors of those works used a simplified model taking into account the interactions only between the nearest neighbors in the δ-layer, but the applicability of this model is not obvious. In this work, to determine the type of the magnetic order in DMAs, we use accurate ab initio calculations of the exchange interaction integrals and total energies of the antiferromagnetic and ferromagnetic configurations, because such an approach is quite reliable when determining the type of the magnetic order.

In addition to germanium and silicon, a disordered solid solution $Si_{0.5}Ge_{0.5}$, where silicon and germanium atoms are randomly distributed over the lattice sites, is considered for the first time as a matrix in the alloys under investigation. In addition to manganese, we also analyze transition metals Ti, V, Cr, Fe, Co, and Ni as δ-doping elements. It is worth noting that the presence (absence) of the local magnetic moment in the bulk transition metals Ti, V, Co, and Ni does not necessarily mean the presence (absence) of the local magnetic moment on an ion of this type in the digital alloy with a Group-IV element.

As was shown in [45], the difference between the energies of intralayer antiferromagnetic and ferromagnetic configurations of local moments in Si/Fe DMAs are sensitive to a change in the shortest bond length between the iron and silicon atoms, appearing in structural relaxation. For this reason, we investigate the intralayer magnetic ordering in digital alloys in both relaxed and unrelaxed systems.

3. DESCRIPTION OF THE MODEL AND CALCULATION METHOD

DMAs were simulated by $A^{IV}{}_7/M$ supercells consisting of a substitutional monolayer of M = Ti, V, Cr, Mn, Fe, Co, or Ni and a semiconductor spacer of A^{IV} = Si, $Si_{0.5}Ge_{0.5}$, or Ge with a thickness of seven atomic layers. According to the calculations of the exchange parameters, the spacer of this thickness weakens the interlayer exchange interactions. For this reason, there are no qualitative differences in the magnetic order in the δ-layers of the $A^{IV}{}_7/M$ and $A^{IV}{}_{11}/M$ DMAs; this conclusion is confirmed by test calculations for A^{IV} = Si, Ge and M = Mn, Fe. A subscript of 7 will be omitted below in the notation $A^{IV}{}_7/M$ except for the cases where this subscript is necessary. The (001) plane was chosen as the growth plane of a DMA. The basis vectors of unit cells, **a**, **b**, and **c**, are directed along [100], [010], and [001], respectively, and their lengths are $a = b = a_0^A$ and $c = 2a_0^A$, where a_0^A is the optimized lattice constant of the bulk Group-IV semiconductor A^{IV} in the diamond structure. The equilibrium parameters of the lattices of semiconductors were determined by finding the extrema of the calculated volume dependences of the total energy fitted to the second-order Birch equation of state [47]. The lattice constants thus obtained are a_0^{Si} = 5.46 Å, $a_0^{Si_{0.5}Ge_{0.5}}$ = 5.61 Å, and a_0^{Ge} = 5.77 Å.

The calculations were carried out in the framework of the electron density functional theory in the generalized gradient approximation to the exchange-correlation potential [48]. To perform structural relaxations in DMAs, we used a plane-wave basis and PAW pseudopotentials [49] implemented in the VASP (Vienna ab initio simulation package) [50, 51]. The basis set of plane waves with energies below 500 eV and the 6 × 6 × 2 Γ-centered grid of special **k**-points [52] ensured the convergence of the total energy with an accuracy of 0.1 meV per atom. When a denser grid was used in the Brillouin zone, the relaxations were changed by no more than 0.25%. The optimization of atomic positions continued until the achievement of forces lower than 0.01 eV/Å for each atom in the superlattice. After that, the electronic structure was calculated by the Korringa–Kohn–Rostoker method [53, 54] in the atomic sphere approximation; as is known, the use of this approximation to investigate systems with high symmetry in the framework of the supercell method gives reasonable results [55]. We also performed test calculations using the full-potential version of the Korringa–Kohn–Rostoker method, which did not reveal significant differences from the calculations in the atomic-sphere approximation for total energies, magnetic moments, and exchange parameters. Since the calculations using the Korringa–Kohn–Rostoker method in the atomic sphere approximation are less expensive, we apply this approximation. A 12 × 12 × 6 grid of special **k**-points is used in the calculations. The total energy calculated with more accurate grids is changed by less than 1 meV per unit cell.

The fully relaxed disordered $Si_{0.5}Ge_{0.5}$ alloy is simulated in the coherent potential approximation formulated in the framework of the Korringa–Kohn–Rostoker method [56, 57]. The correctness of the description of the disordered $Si_{0.5}Ge_{0.5}$ alloy in our calculations is confirmed by satisfactory agreement between the calculated (0.01 Å) and experimental (0.007 Å [58]) values of the deviation of the lattice parameter $a_0^{Si_{0.5}Ge_{0.5}}$ from the value obtained under the assumption of the linear behavior of $a_0^{Si_{1-x}Ge_x}(x)$ (Vegard's law [59]). To optimize the atomic positions in the $Si_{0.5}Ge_{0.5}$/M DMA, we interpolated the shift values observed at relaxations in Si/M and Ge/M according to the calculated dependence $a_0^{Si_{1-x}Ge_x}(x)$.

As is known, the electron density functional theory cannot correctly describe the electronic structures of semiconductors and insulators: this theory underestimates the band gaps. At the same time, the band spec-

tra obtained in the framework of the GW approximation are in good agreement with the experiment [60]. In our calculations, the electronic structures of bulk Si, $Si_{0.5}Ge_{0.5}$, and Ge are fitted to those obtained in the GW approximation [61] using the combined approach [62, 63], where the energy of valence p-electrons of a semiconductor is taken into account by introducing the effective Coulomb potential U, whereas the core and valence s-electrons are described by the generalized gradient approximation potential. Thus, agreement with the GW calculations of the band spectra of Si, $Si_{0.5}Ge_{0.5}$, and Ge is achieved at the effective Coulomb potential magnitudes U = 1.38, 1.25, and 1.53 eV, respectively. In this case, the band gaps correspond to the experimental values $E_g^{Si} \approx 1.12$ eV, $E_g^{Si_{0.5}Ge_{0.5}} \approx 1$ eV (the band gap for the fully relaxed alloy [61]), and $E_g^{Ge} \approx 0.65$ eV.

The calculation of the parameters of the exchange interaction J_{ij} between the local moments of transition metal ions in the alloys was performed on 32 × 32 × 16 grids of **k**-points using the magnetic force theorem [64] and Heisenberg Hamiltonian

$$H = -\sum J_{ij}\mathbf{e}_i \cdot \mathbf{e}_j,$$

where $\mathbf{e}_{i(j)}$ are the unit vectors oriented in the directions of local magnetic moments and J_{ij} describe the interactions between them. The idea of the magnetic force theorem is to consider infinitesimal rotations of classical spins located at two different sites. Energy changes thus appearing, $\delta E = J_0(1 - \cos\delta\theta)$, where $\delta\theta$ is the rotation angle, are mapped onto the classical Heisenberg Hamiltonian using multiple-scattering theory. The coefficient $J_0 = \sum_{i \neq 0} J_{0i}$, which corresponds to the energy required for changing the direction of a local moment to the opposite direction, reflects the "single-site spin stiffness" and the ferromagnetic state is stable when $J_0 > 0$.

4. RESULTS AND DISCUSSION

4.1. Structural Relaxation

In the model used here, the introduction of a transition metal monolayer into the elementary-semiconductor matrix induces such relaxations in which the atomic planes of the semiconductor move as a whole, whereas the in-plane atomic displacements along [001] are negligibly small. This situation is impossible if each atomic plane of the semiconductor spacer contains atoms of two types, as in the case of $Si_{0.5}Ge_{0.5}$. Strictly speaking, the short-range order is absent in the disordered $Si_{1-x}Ge_x$ alloy, because the lengths of Si–Si, Si–Ge, and Ge–Ge interatomic bonds (i.e., the shortest distances) are not the same. In this case, the real positions of silicon and germanium atoms do not correspond to the sites of the ideal diamond structure; this fact, together with the presence of two types of atoms, leads to a more complex character of relaxations in the case of the introduction of the δ-layer of a transition metal into the semiconductor. Unfortunately, the described situation cannot be simulated in the coherent potential approximation. For this reason, in the case of the $Si_{0.5}Ge_{0.5}$/M DMAs, we consider only a certain "average lattice" in which the lengths of the Si–Si, Si–Ge, and Ge–Ge bonds are equal to each other. In the framework of this model, the in-plane displacements of the atoms of the spacer, which are due to the introduction of the transition metal monolayer into the semiconductor, are absent.

The table presents changes in the lengths of the A^{IV}–M interatomic bond in structural relaxations. It can be easily seen that the δ-layer of a particular transition metal (except for Ni) introduced into different matrices induces relaxations of different signs. It is known that the bond lengths in ionic compounds are equal with a high accuracy to the sum of the radii of ions [65]. For the A^{IV}/M digital alloys, which are apparently ionic compounds in the δ-doping region because of the inequality of the electronegativities of the components, this equality can also be valid: $d_{A^{IV}-M} = d_A^{ion} + d_M^{ion}$. Therefore, the lengths of the bonds between atoms of a given transition metal with A^{IV} atoms of different types should really be different, because the radii of ions depend on their charge states, which are determined by the relation between the electronegativities of the elements.

4.2. Local Moments of Transition Metal Ions

The local magnetic moments of transition metal ions entering into various digital alloys are shown in Fig. 1. Considering alloys with nonzero magnetizations, we note that the calculated local moments of transition metal ions in A^{IV}/V, A^{IV}/Cr, A^{IV}/Mn, and Ge/Fe appear to be higher than the values in respective bulk transition metals, whereas these moments in Si/Fe and $Si_{0.5}Ge_{0.5}$/Fe are lower than the respective bulk values. However, it was found that the values of local moments in unrelaxed DMAs A^{IV}/Fe are 16–22% higher than those in relaxed alloys and are no lower than the value in ordinary iron. The last circumstance indicates the well-known relation between the local moments and distances to nearest neighbors (as a rule, atoms of first two coordination spheres). Namely, the magnetic moments on iron ions in relaxed alloys decrease owing to the broadening of iron d-bands, which is induced by a stronger interaction of the electrons of iron with the electrons of spacer atoms and the hybridization of electron states appearing due to a strong decrease in the bond length $d_{A^{IV}-Fe}$ upon relaxation (see table). For the same reason, the local moments of transition metals in most of A^{IV}/M DMAs are higher than the moments in the respective bulk transition metals: the shortest distances d_{M-M} in A^{IV}/M DMAs are much larger than the

Change in the shortest bond length between ions of semiconductor A and transition metal upon structural relaxation

	Unrelaxed DMAs			Relaxed DMAs		
	Si	$Si_{0.5}Ge_{0.5}$	Ge	Si	$Si_{0.5}Ge_{0.5}$	Ge
d_{M-M}, Å	3.865	3.966	4.084	3.865	3.966	4.084
$d_{A^{IV}-Ti}$, Å	2.366	2.429	2.50	2.483	2.509	2.534
$d_{A^{IV}-V}$, Å	2.366	2.429	2.50	2.441	2.465	2.498
$d_{A^{IV}-Cr}$, Å	2.366	2.429	2.50	2.410	2.444	2.496
$d_{A^{IV}-Mn}$, Å	2.366	2.429	2.50	2.390	2.423	2.460
$d_{A^{IV}-Fe}$, Å	2.366	2.429	2.50	2.303	2.341	2.388
$d_{A^{IV}-Co}$, Å	2.366	2.429	2.50	2.272	2.299	2.334
$d_{A^{IV}-Ni}$, Å	2.366	2.429	2.50	2.272	2.296	2.329

respective distances in bulk transition metals comparable with the shortest bond lengths $d_{A^{IV}-M}$ in the considered DMAs.

The A^{IV}/Co alloys whose magnetization surprisingly appears to be zero, except for Ge/Co, are of interest. According to the first Hund's rule, a free cobalt atom, as well as a free vanadium atom, has a magnetic moment of $3\mu_B$. In addition, bulk vanadium, in contrast to cobalt, is nonmagnetic. Nevertheless, vanadium in DMAs with Group-IV elements has a local moment, whereas cobalt has not. Titanium and nickel, which have magnetic moments $2\mu_B$ in the form of free atoms, as well as cobalt, have no local moment in A^{IV}/M digital alloys.

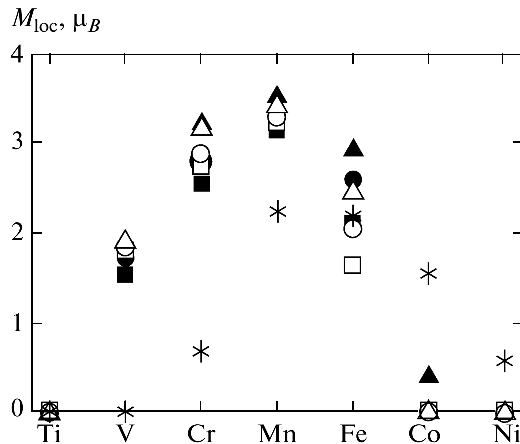

Fig. 1. Local magnetic moments M_{loc} of transition metal ions in DMAs (□, ■) Si/M, (○, ●) $Si_{0.5}Ge_{0.5}$/M, and (△, ▲) Ge/M (open symbols) with and (closed symbols) without taking into account of relaxations. The asterisks show the local magnetic moments in the respective bulk transition metals. For A^{IV}/V and Ge/Gr, the values of M_{loc} in AFM solutions are indicated.

4.3. Magnetic Ordering

When calculating the exchange parameters, we took into account the interactions between local moments spaced by distances of no more than $3a_0^{A^{IV}}$. This cutoff radius covers 11 coordination spheres. The distance between neighboring transition metal monolayers in the considered DMAs is $2a_0^{A^{IV}}$; hence, the magnitudes of the exchange interactions between the spins of neighboring ferromagnetic δ-layer were also estimated in our calculations. The intensity of such superexchange appears to be an order of magnitude less than that of interlayer exchange in agreement with expectations.

As is seen in Figs. 2b, 2c, the ferromagnetic solution studied in $Si_{0.5}Ge_{0.5}$/V and Ge/V is unstable, because the dominant exchange-interaction constants J_{01} are negative. In turn, in view of this circumstance, the single-site spin stiffness coefficient is negative, $J_0 < 0$, and energy is not required for the rotation of the spin (see Figs. 3a, 3b), because the system tends to the energetically favorable antiferromagnetic configuration in which the spins of the nearest neighbors are antiparallel (we refer to this configuration as AFM1). In contrast to $Si_{0.5}Ge_{0.5}$/V and Ge/V, no one of the constants J_{0i} is explicitly dominant for the ferromagnetic configuration of the δ-layer of vanadium in silicon and the constants J_{0i} are very small. The single-site spin stiffness coefficient is also very small, J_0 = 0.62 meV (see Fig. 3a). The calculations of the total energies indicate that the ferromagnetic solution is unfavorable as compared to the AFM1 configuration. In this case, the inconsistency of the signs of J_0 and ΔE

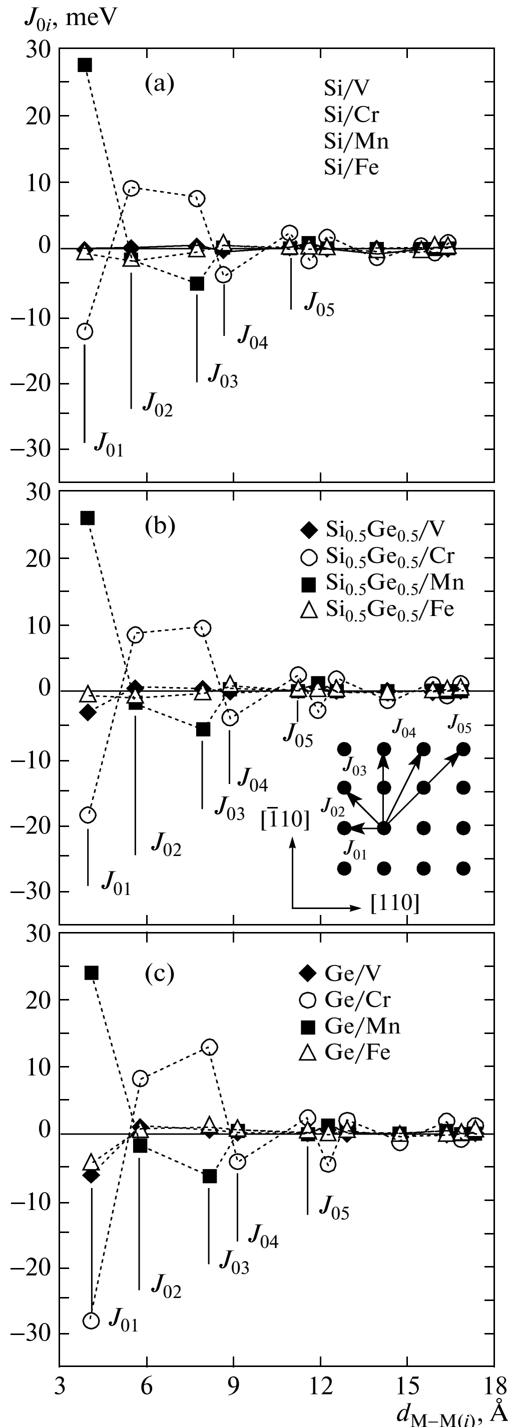

Fig. 2. Exchange integrals J_{0i} calculated for the ferromagnetic solutions in (a) Si/M, (b) $Si_{0.5}Ge_{0.5}$/M, and (c) Ge/M DMAs versus the distance $d_{M-M(i)}$ between a transition metal ion and its ith neighbor. Only intraplane interactions are shown. The inset in panel (b) shows the substitutional δ-layer; the arrows indicate exchange interactions.

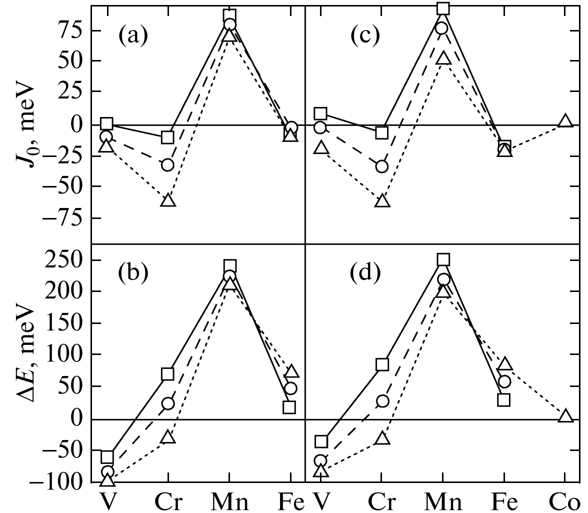

Fig. 3. (a, c) Single-site spin stiffness coefficients J_0 calculated for the ferromagnetic solutions and (b, d) the difference between the total energies of the AFM1 and ferromagnetic configurations $\Delta E = E_{AFM1} - E_{FM}$ for various δ-doping elements and semiconductor matrices (□) Si, (○) $Si_{0.5}Ge_{0.5}$, and (△) Ge. Calculations with and without structural relaxations are shown in panels (a, b) and (c, d), respectively.

is apparently due to strongly different local moments on vanadium ions in the ferromagnetic and AFM1 solutions. The low magnetic moment, $1.12\mu_B$, in the ferromagnetic solution with the positive single-site spin stiffness likely corresponds to a metastable state, whereas the higher moment in the AFM1 solution, $1.82\mu_B$, leads to the dominance of the antiferromagnetic exchange, ensuring a significant energy gain.

The exchange between nearest neighbors in A^{IV}/Cr DMAs has the antiferromagnetic character. However, the ferromagnetic interactions with the second and third neighbors make a significant contribution to the total energy, which prevents the implementation of the AFM1 configuration. This circumstance is manifested in the difference ΔE between the total energies of the AFM1 and ferromagnetic configurations of local moments, see Fig. 3b. It is seen in the figure that the AFM1 configuration is energetically favorable only in Ge/Cr. Nevertheless, the values of the coefficient J_0 for Si/Cr and $Si_{0.5}Ge_{0.5}$/Cr are negative (see Fig. 3a) and an antiferromagnetic configuration with a more complex structure than the AFM1 configuration is more probable than the ferromagnetic configuration in the δ-layer of chromium.

As is seen in Fig. 2, the exchange interaction J_{01} between the nearest neighbors in all systems with manganese monolayers is significantly ferromagnetic and prevails over the interactions with the next coordination spheres. Since the A^{IV}/Mn systems are half-metals or nearly half-metals [40–44], the intensity of the exchange interactions decreases rapidly with an

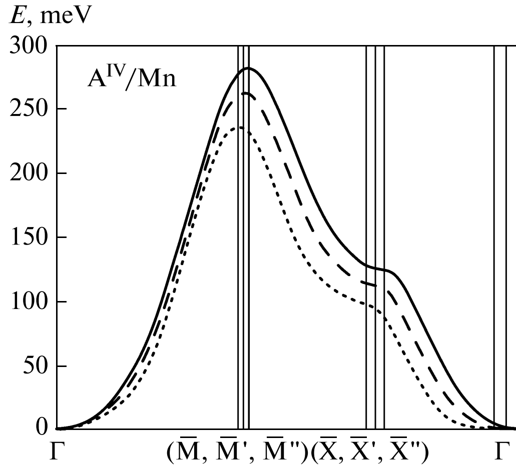

Fig. 4. Magnon spectra calculated for the ferromagnetic solutions in (solid line) Si/Mn, (dashed line) $Si_{0.5}Ge_{0.5}$/Mn, and (dotted line) Ge/Mn alloys. The symmetric points of the Brillouin zone have the following coordinates: $\Gamma = (0, 0)$, $\bar{M} = (\pi/a_0^{Ge}, \pi/a_0^{Ge})$, $\bar{M}' = (\pi/a_0^{Si_{0.5}Ge_{0.5}}, \pi/a_0^{Si_{0.5}Ge_{0.5}})$, $\bar{M}'' = (\pi/a_0^{Si}, \pi/a_0^{Si})$, $\bar{X} = (\pi/a_0^{Ge}, 0)$, $\bar{X}' = (\pi/a_0^{Si_{0.5}Ge_{0.5}}, 0)$, and $\bar{X}'' = (\pi/a_0^{Si}, 0)$.

increase in the distance between local moments in view of the presence of a band gap in the spin-down channel. Positive single-site spin stiffness coefficients J_0, see Fig. 3a, indicate the stable tendency to the formation of the ferromagnetic order in the δ-layers of manganese. This tendency is also confirmed by the calculations of the total energies of the ferromagnetic and AFM1 structures (see Fig. 3b).

Weak exchange interactions and the ground state different from the ferromagnetic one are observed in systems with iron δ-layers. The pictures of exchange interactions in iron monolayers are different for different semiconductor matrices A^{IV}. In particular, the exchange interaction with the second neighbors prevails in the Si/Fe system, $J_{01} = -1.80$ meV (see Fig. 2a), whereas the parameters J_{0i} ($i = 1, 2, 3$) in the $Si_{0.5}Ge_{0.5}$/Fe DMA are quite close to each other (see Fig. 2b). In both cases, the probability of the establishment of a complex magnetic structure is high, because the J_0 values obtained are negative, whereas ΔE values are positive. In the Ge/Fe system, the value $J_{01} = -4.62$ meV is remarkable and, since $J_0 = -17.9$ meV, it is reasonable to assume that the AFM1 configuration is energetically more favorable than the ferromagnetic configuration, but the calculations of the total energies indicate that this is not the case. Thus, a complex antiferromagnetic structure is also implemented in the Ge/Fe DMA.

For A^{IV}/Mn DMAs, we also calculated the total energies of paramagnetic (PM) phases, which were simulated in the disordered local moment approximation. For the other alloys, the energies of the ferromagnetic and paramagnetic phases were not compared, because the ferromagnetic order in them is either energetically unfavorable or unstable. It appears that the ferromagnetic solution is more favorable than the paramagnetic solution by 124, 118, and 111 meV for the Si/Mn, $Si_{0.5}Ge_{0.5}$/Mn, and Ge/Mn DMAs, respectively.

To analyze the stability of the ferromagnetic order in the δ-layers of manganese, we calculated the magnon spectra for corresponding DMAs, see Fig. 4. It is worth noting that the magnon spectrum of a particular system is meaningful only if it corresponds to the ground state, which is known, e.g., from the experiment. According to the calculations of the total energies and especially exchange integrals, the ferromagnetic solution in A^{IV}/Mn DMAs is stable; consequently, it is reasonable to assume that this state is the ground state. As is seen in Fig. 4, the ferromagnetic solution is dynamically stable in all three systems, because the spectra are in the region of positive energies. Moreover, the maxima of the spectra are at the symmetric points of the Brillouin zones, indicating that the magnetic structure in manganese monolayers is collinear. The ferromagnetic solution in the Si/Mn alloy is most stable, because the energies of the magnon spectrum at the symmetric points M" and X" for it are maximal and the dispersion curves increase most rapidly in the Γ–M" and Γ–X" directions, respectively. These facts are in agreement with the data that are shown in Figs. 2 and 3 and indicate that J_0 and ΔE values are maximal for Si/Mn.

As was mentioned in the Introduction, it was reported in [44] that the ferromagnetic configuration of local moments in the δ-layer of the unrelaxed Si_{23}/Fe DMA is energetically less favorable than the AFM1 configuration. According our calculations of the total energies for unrelaxed DMAs, the energy of the ferromagnetic configuration in the Si_7/Fe alloy is lower than that of the AFM1 configuration, $\Delta E = E_{AFM1} - E_{FM} > 0$ (see Fig. 3d). It is noteworthy that the comparison of the ΔE values for $A^{IV}{}_7$/M and $A^{IV}{}_{23}$/M is possible, because the interlayer exchange interactions are disregarded in the calculations of the total energies (supercells under consideration contain one δ-layer of the transition metal). Significant differences between the ΔE values for unrelaxed $A^{IV}{}_7$/M and $A^{IV}{}_{23}$/M DMAs (A^{IV} and M are the same for both alloys) are generally not expected. However, in order to improve the description of the electronic structure of Group-IV semiconductors, we described their *p*-states with the generalized gradient approximation potential supplemented by the effective Coulomb potential *U*, whereas *p*-states in [44] was described only with the generalized gradient approximation potential. Consequently, it would be more correct to

compare the calculations performed in the framework of the "pure" generalized gradient approximation. However, the ΔE value calculated with $U = 0$ is also positive, 33 meV per Fe atom. Thus, discrepancy with the result obtained in [44] is due not to the use of the potential U, but to other factors. In view of this circumstance, it is worth noting that it is impossible to correctly compare these contradictory results and to discuss possible causes of differences, because the authors of [44] did not present the lattice parameter of silicon used in the calculations and its band gap, as well as did not indicate the grid of **k**-points used for integration over the Brillouin zone.

Figures 3c and 3d show the parameters J_0 and the differences ΔE between the energies of the AFM1 and ferromagnetic solutions for unrelaxed A^{IV}/M DMAs. The comparison of J_0 values with their values after relaxation for, e.g., Si/Mn indicates that J_0 decreases by about 5 meV when the Si–Mn distance increases by 0.03 Å (see Figs. 3a, 3c and table). Considering the δ-layer of manganese in the germanium matrix, it can be seen that the Ge–Mn distance decreases after relaxation, whereas the stability of the ferromagnetic state increases. Relaxations are almost absent in the $Si_{0.5}Ge_{0.5}/Mn$ system and the intensity of the ferromagnetic interaction in the manganese monolayer remains unchanged. Thus, the intensity of exchange interactions between the local moments of manganese ions in the δ-layer depends on the distance d_{Mn-A}. The analysis of differences between the J_0 values before and after relaxations for all other DMAs indicates that a decrease in the distance between atoms of the spacer and δ-layer promotes enhancement (weakening) of the ferromagnetic (antiferromagnetic) interaction.

5. CONCLUSIONS

Ab initio calculations constitute one of the most efficient methods for theoretical investigation of the magnetic order in A^{IV}/M DMAs. The simultaneous inclusion of intra- and interlayer exchange interactions obviously makes such a calculation very difficult even for a moderate thickness of the A^{IV} spacer between the δ-layers of transition metals. However, the interlayer exchange interaction in the overwhelming number of DMAs is an order of magnitude weaker than the intralayer exchange interaction even at a thickness of the semiconductor spacer more than three or four atomic layers. As was shown analytically in [35, 36], the effective integral of the interlayer exchange in DMAs changes sing at a certain characteristic thickness of the spacer: at small and large distances between δ-layers, their orientations are parallel (i.e., ferromagnetic) and antiparallel (antiferromagnetic), respectively. When investigating the magnetic and transport properties of DMAs, both situations are of interest and the required magnetic configuration can be realized by choosing the corresponding thickness of the A^{IV} semiconductor spacer. We focus exclusively on the formation of the magnetic order inside the δ-layer and, for simplicity, neglect the effect of interlayer exchange on intralayer exchange. In this formulation of the problem, we could correctly consider only such DMAs in which the distance between neighboring δ-layers of transition metals is much larger than the distance between the transition metal ions inside one δ-layer. In the opposite limit, where these distances are close to each other, our approach is evidently inapplicable.

In order to improve the description of the electronic structure of Group-IV semiconductors, we introduced the effective Coulomb potential as a parameter into the calculations. To determine the effect of this parameter on the calculation of the properties of DMAs, we performed the optimization of the volume of pure silicon and relaxation of the Si/Fe DMA in the generalized gradient approximation for $U = 0$ and a number of values $U \leq 1.38$ eV. The Si/Fe system was taken for the test because of significant structural relaxations. In addition, the data for Si/Fe were already reported in [44].

The calculation results indicate insignificant differences between the structure parameters obtained with $U = 0$ and $U \neq 0$. In particular, the Si–Si bond length in bulk silicon obtained with $U = 1.38$ eV decreases by less than 1%. The lattice parameter of bulk silicon calculated with $U = 1.38$ eV is 5.46 Å, which is larger than the experimental value by only 0.5%. Under structural relaxation in Si/Fe, the shortest Si–Fe bond length calculated with $U = 1.38$ eV increases by less than 0.7%. Thus, the used effective Coulomb potential U very slightly changes the structure properties of the studied DMAs. This is not surprising, because $U = 1.38$ eV is much smaller than the width of the valence band of Group-IV semiconductors (~12 eV).

However, the introduction of U significantly improves the energy spectrum of a semiconductor near the Fermi level, leading to a more correct description of the magnon spectra of DMAs and critical temperatures. We have performed systematic calculations of the exchange parameters J_{0i} for Si/Fe and Si/Mn and revealed that their values are very sensitive to U, i.e., to the band gap in a semiconductor; this property is important for the determination of the most stable magnetic configuration in the δ-layers of DMAs.

The magnetic force theorem [64] was widely discussed [66]. Since this theorem requires the knowledge of only single-particle energies, its applicability, together with the Coulomb parameterization, is doubtless. In our approach, we used the Lloyd formula [64], which allows for the calculation of change in the energy of electrons under small deviations of magnetic moments from their directions in the initial state. Such an approach makes it possible to analyze all possible configurations and, therefore, is a powerful tool for investigating the magnetic order.

To conclude, performing ab initio calculations, we have investigated intralayer magnetic ordering in digital alloys of Si, Ge, and $Si_{0.5}Ge_{0.5}$ with 3*d*-metals Ti, V, Cr, Mn, Fe, Co, and Ni. According to the calculations of exchange interaction integrals, total energies, and magnon spectra, stable intralayer ferromagnetism occurs only in the systems with Mn δ-layers, whereas this ferromagnetism in DMAs based on V, Cr, and Fe is unstable. The antiferromagnetic configuration with antiparallel spins of nearest neighbors in the doping δ-layer likely occurs in the monolayers of Si/V, Ge/V, $Si_{0.5}Ge_{0.5}$/V, and Ge/Cr, whereas monolayers of all other alloys exhibit the tendency to the formation of more complex antiferromagnetic configurations except for the systems with Ti, Co, and Ni δ-layers in which there are no magnetic interactions for all considered variants of semiconductor matrices.

In view of the above results, we attract attention to the following fact. A significant advance has been recently achieved in obtaining modulation-doped heterostructures Si_xGe_{1-x} with strained Ge serving as a conducting channel, which have very high drift mobilities of holes (about 3000 $cm^2/(V\ s)$) [67]. According to our calculations, hypothetical heterostructures (Si_xGe_{1-x}/δ-Mn)/Si_xGe_{1-x}/Ge, which contain a ferromagnetic layer (Si_xGe_{1-x}/Mn DMA) and a conducing channel (strained Ge layer) spatially separated by a Si_xGe_{1-x} layer, can become promising for the implementation of the effective transport of spin-polarized carriers (holes). Such a heterostructure can simultaneously exhibit the stable ferromagnetic order in Si_xGe_{1-x}/Mn DMAs, the high mobility of holes, and their high spin polarization in the Ge conducting channel owing to the magnetic proximity of the channel to the ferromagnetic δ-layer. Similar effects were earlier detected in (GaAs/δ-Mn)/GaAs/InGaAs [68, 69].

ACKNOWLEDGMENTS

The calculations were performed on the SKIF Cyberia computational cluster (Tomsk). We are grateful to V.N. Men'shov for stimulating discussions and to E.T. Kulatov for critical comments. This work was supported in part by the Ministry of Education and Science of the Russian Federation, Federal Targeted Program "Scientific and Scientific-Pedagogical Personnel of Innovative Russia in 2009–2013," and by the Russian Foundation for Basic Research, project no. 10-02-00118.

REFERENCES

1. I. Žutić, J. Fabian, and S. Das Sarma, Rev. Mod. Phys. **76**, 323 (2004).
2. A. Stroppa, S. Picozzi, A. Continenza, and A. J. Freeman, Phys. Rev. B: Condens. Matter **68**, 155203 (2003); S. Picozzi, F. Antoniella, A. Continenza, A. Mosca Conte, A. Debernardi, and M. Peressi, Phys. Rev. B: Condens. Matter **70**, 165 205 (2004).
3. Y. D. Park, A. T. Hanbicki, S. C. Erwin, C. S. Hellberg, J. M. Sullivan, J. E. Mattson, T. F. Ambrose, A. Wilson, G. Spanos, and B. T. Jonker, Science (Washington) **295**, 651 (2002).
4. S. Ahlers, D. Bougeard, N. Sircar, G. Abstreiter, A. Trampert, M. Opel, and R. Gross, Phys. Rev. B: Condens. Matter **74**, 214411 (2006).
5. A. I. Dmitriev, R. B. Morgunov, O. L. Kazakova, and Y. Tanimoto, Zh. Eksp. Teor. Fiz. **135** (6), 1134 (2009) [JETP **108** (6), 985 (2009)].
6. C. Jaeger, C. Bihler, T. Vallaitis, S. T. B. Goennenwein, M. Opel, R. Gross, and M. S. Brandt, Phys. Rev. B: Condens. Matter **74**, 045330 (2006).
7. E. Biegger, L. Stäheli, M. Fonin, U. Rüdiger, and Yu. S. Dedkov, J. Appl. Phys. **101**, 103912 (2007).
8. A. P. Li, J. F. Wendelken, J. Shen, L. C. Feldman, J. R. Thompson, and H. H. Weitering, Phys. Rev. B: Condens. Matter **72**, 195205 (2005).
9. S. Cho, S. Choi, S. C. Hong, Y. Kim, J. B. Ketterson, B.-J. Kim, Y. C. Kim, and J.-H. Jung, Phys. Rev. B: Condens. Matter **66**, 033303 (2002).
10. W. Gao, D. Hou, Y. Hu, and S. Wei, Solid State Commum. **149**, 1924 (2009).
11. R. R. Gareev, Yu. V. Bugoslavsky, R. Schreiber, A. Paul, M. Sperl, and M. Döppe, Appl. Phys. Lett. **88**, 222508 (2006).
12. F. M. Zhang, X. C. Liu, J. Gao, X. S. Wu, Y. W. Du, H. Zhu, J. Q. Xiao, and P. Chen, Appl. Phys. Lett. **85**, 786 (2004).
13. M. Bolduc, C. Awo-Affouda, A. Stollenwerk, M. B. Huang, F. G. Ramos, G. Agnello, and V. P. LaBella, Phys. Rev. B: Condens. Matter **71**, 033302 (2005).
14. X. C. Liu, Z. H. Lu, Z. L. Lu, L. Y. Lv, X. S. Wu, F. M. Zhang, and Y. W. Du, J. Appl. Phys. **100**, 073903 (2006).
15. X. C. Liu, Y. B. Lin, J. F. Wang, Z. H. Lu, Z. L. Lu, J. P. Xu, L. Y. Lv, F. M. Zhang, and Y. W. Du, J. Appl. Phys. **102**, 033902 (2007).
16. L. Zeng, E. Helgren, M. Rahimi, F. Hellman, R. Islam, B. J. Wilkens, R. J. Culbertson, and D. J. Smith, Phys. Rev. B: Condens. Matter **77**, 073306 (2008).
17. A. Wolska, K. Lawniczak-Jablonska, M. Klepka, and M. S. Walczak, Phys. Rev. B: Condens. Matter **75**, 113201 (2007).
18. S. Zhou, K. Potzger, G. Zhang, A. Mücklich, F. Eichhorn, N. Schell, R. Grötzschel, B. Schmidt, W. Skorupa, M. Helm, J. Fassbender, and D. Geiger, Phys. Rev. B: Condens. Matter **75**, 085203 (2007).
19. C. Awo-Affouda, M. Bolduc, M. B. Huang, F. Ramos, K. A. Dunn, B. Thiel, G. Agnello, and V. P. LaBella, J. Vac. Sci. Technol., A **24** (4), 1644 (2006).

20. S. Zhou, A. Shalimov, K. Potzger, M. Helm, J. Fassbender, and H. Schmidt, Phys. Rev. B: Condens. Matter **80**, 174423 (2009).

21. S. N. Nikolaev, B. A. Aronzon, V. V. Ryl'kov, V. V. Tugushev, E. S. Demidov, S. A. Levchuk, V. P. Lesnikov, V. V. Podol'skii, and R. R. Gareev, Pis'ma Zh. Eksp. Teor. Fiz. **89** (12), 707 (2009) [JETP Lett. **89** (12), 603 (2009)].

22. W. F. Su, L. Gong, J. L. Wang, S. Chen, Y. L. Fan, and Z. M. Jiang, J. Cryst. Growth **311** (7), 2139 (2009).

23. U. Gottlieb, A. Sulpice, B. Lambert-Andron, and O. Laborde, J. Alloys Compd. **361**, 13 (2003); A. Sulpice, U. Gottlieb, M. Affronte, and O. Laborde, J. Magn. Magn. Mater. **272**, 519 (2004).

24. M. Lee, Y. Onose, Y. Tokura, and N. P. Ong, Phys. Rev. B: Condens. Matter **75**, 172 403 (2007).

25. A. F. Orlov, A. B. Granovsky, L. A. Balagurov, I. V. Kulemanov, Yu. N. Parkhomenko, N. S. Perov, E. A. Gan'shina, V. T. Bublik, K. D. Shcherbachev, A. V. Kartavykh, V. I. Vdovin, A. Sapelkin, V. V. Saraikin, Yu. A. Agafonov, V. I. Zinenko, A. Rogalev, and A. Smekhova, Zh. Eksp. Teor. Fiz. **136** (4), 703 (2009) [JETP **109** (4), 602 (2009)].

26. R. K. Kawakami, E. Johnston-Halperin, L. F. Chen, M. Hanson, N. Guebels, J. S. Speck, A. C. Gossard, and D. D. Awschalom, Appl. Phys. Lett. **77**, 2379 (2000).

27. T. C. Kreutz, G. Zanelatto, E. G. Gwinn, and A. C. Gossard, Appl. Phys. Lett. **81**, 4766 (2002).

28. H. Luo, B. D. McCombe, M. H. Na, K. Mooney, F. Lehmann, X. Chen, M. Cheon, S. M. Wang, Y. Sasaki, X. Liu, and J. K. Furdyna, Physica E (Amsterdam) **12**, 366 (2002).

29. X. Chen, M. Na, M. Cheon, S. Wang, H. Luo, B. D. McCombe, X. Liu, Y. Sasaki, T. Wojtowicz, J. K. Furdyna, S. J. Potashnik, and P. Schiffer, Appl. Phys. Lett. **81**, 511 (2002).

30. B. D. McCombe, M. Na, X. Chen, M. Cheon, S. Wang, H. Luo, X. Liu, Y. Sasaki, T. Wojtowicz, J. K. Furdyna, S. J. Potashnik, and P. Schiffer, Physica E (Amsterdam) **16**, 90 (2003).

31. A. M. Nazmul, S. Sugahara, and M. Tanaka, Phys. Rev. B: Condens. Matter **67**, 241 308(R) (2003).

32. A. M. Nazmul, S. Kobayashi, S. Sugahara, and M. Tanaka, Physica E (Amsterdam) **21**, 937 (2004).

33. S. H. Chiu, H. S. Hsu, and J. C. A. Huang, J. Appl. Phys. **103**, 07D110 (2008).

34. T. Moriya, *Spin Fluctuations in Itinerant Electron Magnetism* (Springer, Berlin, 1985; Mir, Moscow, 1988).

35. V. N. Men'shov and V. V. Tugushev, Zh. Eksp. Teor. Fiz. **133** (5), 1070 (2008) [JETP **106** (5), 936 (2008)].

36. V. N. Men'shov, V. V. Tugushev, P. M. Echenique, S. Caprara, and E. V. Chulkov, Phys. Rev. B: Condens. Matter **78**, 024438 (2008).

37. S. Caprara, V. V. Tugushev, P. M. Echenique, and E. V. Chulkov, Europhys. Lett. **85**, 27006 (2009).

38. V. N. Men'shov, V. V. Tugushev, S. Caprara, P. M. Echenique, and E. V. Chulkov, Phys. Rev. B: Condens. Matter **80**, 035315 (2009).

39. A. Continenza, F. Antoniella, and S. Picozzi, Phys. Rev. B: Condens. Matter **70**, 035310 (2004).

40. H. Y. Wang and M. C. Qian, J. Appl. Phys. **99**, 08D705 (2006).

41. S. Picozzi, M. Ležaić, and S. Blügel, Phys. Status Solidi A **203** (11), 2738 (2006).

42. M. C. Qian, C. Y. Fong, K. Liu, W. E. Pickett, J. E. Pask, and L. H. Yang, Phys. Rev. Lett. **96**, 027211 (2006).

43. C. Y. Fong, M. Shauhgnessy, R. Snow, and L. H. Yang, Phys. Status Solidi C **7**(3–4), 747 (2010).

44. Yu. A. Uspenskii and E. T. Kulatov, J. Magn. Magn. Mater. **321**, 931 (2009).

45. M. M. Otrokov, S. A. Ostanin, A. Ernst, V. M. Kuznetsov, and E. V. Chulkov, Fiz. Tverd. Tela (St. Petersburg) **52** (8), 1563 (2010) [Phys. Solid State **52** (8), 1680 (2010)].

46. H. Wu, P. Kratzer, and M. Scheffler, Phys. Rev. Lett. **98**, 117202 (2007).

47. F. Birch, J. Geophys. Res. **57**, 227 (1952).

48. J. P. Perdew and W. Wang, Phys. Rev. B: Condens. Matter **45**, 13244 (1992).

49. P. E. Blöchl, Phys. Rev. B: Condens. Matter **50**, 17953 (1994).

50. G. Kresse and J. Fürthmuller, Phys. Rev. B **54**, 11169 (1996).

51. G. Kresse and J. Joubert, Phys. Rev. B: Condens. Matter **59**, 1758 (1999).

52. H. J. Monkhorst and J. D. Pack, Phys. Rev. B: Solid State **13**, 5188 (1976).

53. J. Korringa, Physica (Amsterdam) **13**, 392 (1947).

54. W. Kohn and N. Rostoker, Phys. Rev. **94**, 1111 (1954).

55. N. Papanikolaou, R. Zeller, and P. H. Dederichs, J. Phys.: Condens. Matter. **14**, 2799 (2002).

56. P. Soven, Phys. Rev. **156**, 809 (1967).

57. B. L. Gyorffy, Phys. Rev. B: Solid State **5**, 2382 (1972).

58. J. P. Dismukes, L. Ekstrom, and R. J. Paff, J. Phys. Chem. **68**, 3021 (1964).

59. L. Vegard, Z. Phys. **5**, 17 (1921).

60. W. G. Aulbur, L. Jonsson, and J. W. Wilkins, Solid State Phys. **54**, 1 (2000).

61. D. Rideau, M. Feraille, L. Ciampolini, M. Minondo, C. Tavernier, H. Jaouen, and A. Ghetti, Phys. Rev. B: Condens. Matter **74**, 195208 (2006).

62. V. I. Anisimov, J. Zaanen, and O. K. Andersen, Phys. Rev. **44**, 943 (1991).

63. S. L. Dudarev, G. A. Botton, S. Y. Savrasov, C. J. Humphreys, and A. P. Sutton, Phys. Rev. B: Condens. Matter **57**, 1505 (1998).

64. A. Liechtenstein, M. Katsnelson, V. Antropov, and V. Gubanov, J. Magn. Magn. Mater. **67**, 65 (1987).

65. B. K. Vainshtein, V. M. Fridkin, and V. L. Indenbom, *Modern Crystallography*, Vol. 2: *Structure of Crystals* (Nauka, Moscow, 1979; Springer, Berlin, 1982).
66. P. Bruno, Phys. Rev. Lett. **90**, 087 205 (2003).
67. M. Myronov, K. Sawano, Y. Shiraki, T. Mouri, and K. M. Itoh, Appl. Phys. Lett. **91**, 082108 (2007).
68. B. A. Aronzon, V. A. Kul'bachinskii, P. V. Gurin, A. B. Davydov, V. V. Ryl'kov, A. B. Granovski, O. V. Vikhrova, Yu. A. Danilov, B. N. Zvonkov, Y. Horikoshi, and K. Onomitsu, Pis'ma Zh. Eksp. Teor. Fiz. **85** (1), 32 (2007) [JETP Lett. **85** (1) 27 (2007)]; B. A. Aronzon, A. S. Lagutin, V. V. Ryl'kov, V. V. Tugushev, V. N. Men'shov, A. V. Lashkul, R. Laiho, O. V. Vikhrova, Yu. A. Danilov, and B. N. Zvonkov, Pis'ma Zh. Eksp. Teor. Fiz. **87** (3), 192 (2008) [JETP Lett. **87** (3), 164 (2008)]; M. A. Pankov, B. A. Aronzon, V. V. Rylkov, A. B. Davydov, E. Z. Meilikhov, R. M. Farzetdinova, E. M. Pashaev, M. A. Chuev, I. A. Subbotin, I. A. Likhachev, B. N. Zvonkov, A. V. Lashkul, and R. Laiho, Zh. Eksp. Teor. Fiz. **136** (3), 346 (2009) [JETP **109** (2), 293 (2009)]; B. A. Aronzon, M. A. Pankov, V. V. Rylkov, E. Z. Meilikhov, A. S. Lagutin, E. M. Pashaev, M. A. Chuev, V. V. Kvardakov, I. A. Likhachev, O. V. Vihrova, A. V. Lashkul, E. Lähderanta, A. S. Vedeneev, and P. Kervalishvili, J. Appl. Phys. **107**, 023905 (2010).
69. S. V. Zaitsev, V. D. Kulakovskii, M. V. Dorokhin, Yu. A. Danilov, P. B. Demina, M. V. Sapozhnikov, O. V. Vikhrova, and B. N. Zvonkov, Physica E (Amsterdam) **41**, 652 (2009).

Translated by R. Tyapaev